2.5D Technology based on Vertically Aligned Carbon Nanotubes for MM-Waves Passive Devices

Simon Chun Kiat Goh[1,2*], Chun Fei Siah[2*], Joseph De Saxce[3*], Zhikai Ng[2*], Li Lynn Shiau[4], Lucas Lum Yun Xiang[1,2,5], Chong Wei Tan[1,2], Edwin Hang Tong Teo[2,4], Philippe Coquet[1,2,6], Dominique Baillargeat[7], Beng Kang Tay[1,2]

[1]CNRS-NTU-THALES UMI 3288 CINTRA, RTP, Nanyang Technological University, Singapore
[2]School of Electrical and Electronic Engineering, Nanyang Technological University, Singapore
[3]XLIM, CNRS, University of Limoges, UMR 7252, France
[4]Temasek Laboratories, Nanyang Technological University, Singapore
[5]Excelitas Technologies, Singapore
[6]IEMN, CNRS UMR 8520-Universite de Lille, France
[7]CNRS@CREATE Ltd, Singapore
dominique.baillargeat@cnrs.fr

***Abstract*—An original 2.5 technology based on vertically aligned Carbon Nanotubes (VACNTs) to produce millimeter-waves Air-Filled WaveGuide (AFWG) structures is described in this paper. The design of AFWG is based on bundle of VACNTs acting as WG's metallic lateral walls. A CMOS compatible CNTs process is developed to fabricate the WG using a dedicated assembly process. Raman spectroscopy and molecular dynamics are applied to study the effects of the CNTs compression during the fabrication process. An example of the realization of a V band AFWG is presented together with S-parameters measurements which validate the concept of VACNTs-based AFWG. In addition, the experimental attenuation constant is estimated at 0.5 dB/mm between 81–86 GHz.**

***Keywords*—Air-Filled Waveguide, mm-wave, CNTs, Nano-packaging**

I. Introduction

Telecom communities prepare already the beyond-5G to 6G, and present KPIs going to a peak data rate of 1Tb/s (50 times the peak data rate of 5G), space multiplexing, spectrum agility, dense Massive multiple-input multiple-output (MIMO), wide bands, and so forth. To achieve Tb/s transmissions in 6G, it is necessary to use the frequency band over 100GHz or sub-THz due to enormous amount of available bandwidth. However, the use of such high frequency bands results in more design challenges of RF circuits and heterogeneous integrations, in a 3D approach in general.

At these frequencies, there is therefore a need for a new type of low-cost, high performance, integrated passive devices to compete respectively electrical performances and cost of fabrication of 2D [1] and classical 3D technologies.

In this context, the purpose of this work is to propose an alternative and disruptive 2.5D technology based on vertical aligned carbon nanotubes (VACNTs). This technology offers an ease in fabricating patterned CNTs based structures, with any type of geometry and high resolution, together with CNTs' superior physical properties. The use of CNTs is interesting because of the presence of the sp_2 carbon bonds, they have excellent optical, mechanical, thermal and electronic properties [2]. As such, many applications including, RF microelectronics, field emitters, super capacitors, nanopackaging, etc [3-7] have been found. A proof of concept of the realization of a VACNTS-based AFWG for 5G backhaul applications in the 81-86 GHz band is presented in this paper. The proposed structure is easily compatible with a 3D heterogeneous integration, compact, easy to fabricate for low-cost production, potentially low loss for better connectivity, etc.

This article is organized as follows: in Section II the fabrication process is described, in section III the effects of CNTs' compressive deformation are studied, in section IV VACNTS-based AFWG is described, designed and experimentally validated.

II. Fabrication Process

In this study, we propose the followings: (1) replacing classic lateral metal walls of WG structures with carbon nanotubes (CNTs) walls, transferred to the top of metallic layer with (2) the established CNT low temperature transfer technology [6] to solve the mechanical limitation and (3) using air as the propagation medium to reduce the dielectric losses.

Up to now, the biggest challenge for the integration of vertical aligned CNT into electrical circuit has been the high CNT synthesis temperature (>650 °C) and the poor adhesion between synthesized CNTs and supporting substrates, which have greatly restricted the application of CNTs. In this context, a reliable and CMOS-compatible method to precisely transfer and bond vertical CNT arrays at low temperature, less than 300°C, thus overcoming the limitations mentioned above have been developed recently [8]. In this work, the CNTs are grown by a FirstNano CVD system which can grow very high quality VACNTs arrays at lengths up to 4mm. After growth, these CNTs are transferred to the desired substrate by the patented CNT transfer technology [6], as described in Fig. 1. When compared to direct CNT growth, this transfer technology has the advantages of (1) low process_temperature <300°C, (2)

[*] equal contribution

smooth metal surface after processing (3) no amorphous carbon residue that shorts the contact lines and (4) stronger adhesion of the CNTs onto the substrate, (5) "add-on" technology. The fabrication process is summarized in Figure 1:
Step 1: growth of VACNTs with the desired pattern on a separate Si substrate, Step 2: deposition of low melting point metal on top of the VACNT, Step 3: gold layer deposition on a Si wafer for the realization of the cover, Step 4: bonding of the patterned CNTs on the gold plated cover by thermocompression using flip chip, Step 5: release of the patterned CNTs from their original substrate, Step 6: fabrication of the CPW feeding lines on the bottom substrate, Step 7: bonding of the patterned transferred CNTs on the cover to the bottom substrate.

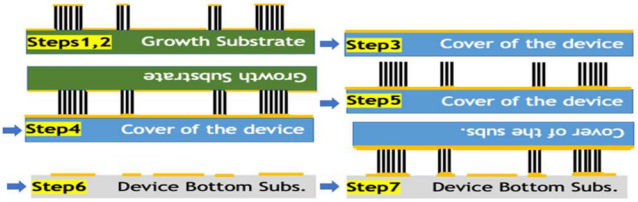

Fig.1. Schematic of the fabrication process

III. Effects of CNTs Compressive Deformation

A. *Raman spectroscopy*

As explained above, during the fabrication process VACNT grown on Si wafers are transferred by thermocompression metal diffusion bonding onto a host substrate to form the AFWG. Then, those VACNT are subjected to axial compression during the transfer process. To control the final height of the WG and to limit the amount of axial deformation, incompressible spacers of (300, 500 and 620 µm are used. This is so because tall CNT are prone to deformation when subjected to external perturbations such as axial tensile / compression, bending, etc [9, 10].

Raman spectroscopy is a typical go-to process for the characterization of material properties [11]. Thus, it is carried out to understand the properties of the VACNT after transfer. The Raman spectra for the transferred samples of VACNT are as shown in Figure 2. The G peak presents at about 1580 cm^{-1} corresponds to the carbon sp2 bending mode [12]. On the contrary, the D peak which exists at about 1350 cm^{-1} is attributed to presence of defects [13]. Therefore, the intensity of the D peak could suggest the amount of defects present. In the first instance, VACNT are terminated after a growth period of 30 min with a height of about 930 µm. These VACNT are then subjected to compression limited by spacers of different heights. As listed, the spacers in use are, 300, 500 and 620 µm. In this case, shorter spacers allow the VACNT to be compressed more. As such, the calculated I_D/I_G ratio for samples compressed with 300, 500 and 620 µm height spacers are 0.783, 0.736 and 0.714, respectively. In the next instance, VACNT are grown with different durations (20, 30 and 40 mins) to achieve different VACNT of height (712, 930, 1180 µm). These VACNTs are compressed to a final height of 300 µm and are then compared. The obtained I_D/I_G ratios are 0.783, 0.783 and 0.971, for 20, 30 and 40 min grown VACNT, respectively. A higher value signifies the presence of a larger defect density. The value corroborates with the fact that higher compression ratio, achieved by longer VACNT growth height or compressed with shorter spacer, would induce more defects on the resulting VACNT.

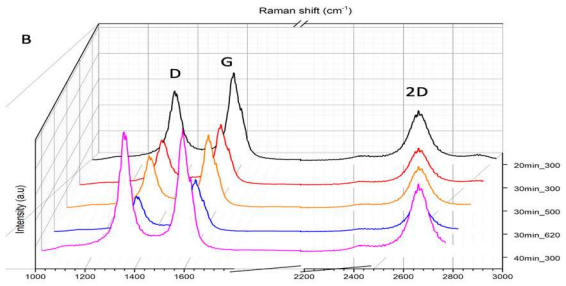

Fig.2. Raman shift of grown VACNT (20, 30 and 40 mins growth time) and height of compression limiting spacers (300, 500 and 620 µm).

Typically, CNTs are minimally impacted by elastic deformation. However, plastic deformations may result in the formation of columnar, shell walled and crimp structures [14] that can occur an increase in sp3 carbon bonds density. In addition, the transfer process definitively involves the elements of elevated pressure and temperature. Consequently, some of the sp2 carbon bonds might have been damaged in the process resulting in the increase in sp3 density as well as the formation of bulb-like structures as shown in Fig 3.

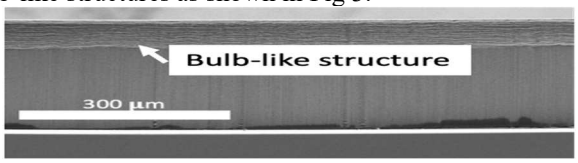

Fig.3. Formation of bulb-like structures due to damaged sp2 carbon bonds during the transfer process

B. *Molecular dynamics reaction force field*

In addition to the Raman spectroscopy study, we aim to understand by simulation the effects of the physical deformation of the VACNT in the direction of stress due to the axial compression. To understand the buckling effect of CNT, molecular dynamics, finite element, Euler buckling theory have been carried out over the past decade [15]. In this work, molecular dynamics simulation was carried out using SCM Amsterdam Suite package with double wall CNT (DWCNT) to simulate the deformation characteristics of multiwall CNT [16]. Firstly, VACNT deformation is carried out using the reaction force field (Reaxff package, CHO.ff) developed for hydrocarbons oxidation [17]. Prior to simulation, 100 000 steps with 0.25 fs/step are set with (Nosé-Hoover chain) NHC thermostat at 5K and a damping constant of 100 fs. Axial compression parameters of 0, -0.00002, -0.00005, -0.0008, -0.0001 and -0.0002 Å/fs are inputted to replicate actual deformation of VACNT under strain. Once completed, a geometrical optimization step is carried out with self-consistent-charge density- functional tight-binding method (SCC-DFTB) model and 3ob-3-1 parameter [16]. The gradient, energy and step convergence are set to 0.001 Hartree / Å and E-5 Hartree and 0.01 Å, respectively. Finally, to extract the electronic properties of the VACNT, the Non-equilibrium

Green function (NEGF) is modelled using the SCC-DFTB and 3ob-3-1 parameter directory. The connecting leads on both ends are set with one repeating unit of DWCNT. In this case, the leads are configured to not deform the simulation. At the same time, the central region is connected to the leads with a fixed bond length of 154 pm. The transmission energy grid is then set between -2 and 2 eV.

This study serves to visualize the outcome of the compressive strain and the electronic properties of a double layer VACNT before and after deformation. We first consider the case of CNTs without defect. As shown in Figure 4, defect-free CNT without external perturbation shows staircase transmission characteristics. Interestingly, with the introduction of a mild compression transmission level between -2 and 2 eV increases by at least 50 %. However, further increase in strain results in the loss of degeneracy as well as a significant decrease in transmission. Despite the marked drop in transmission, an axially strained level between 2 and 30 % does not result in zero transmission.

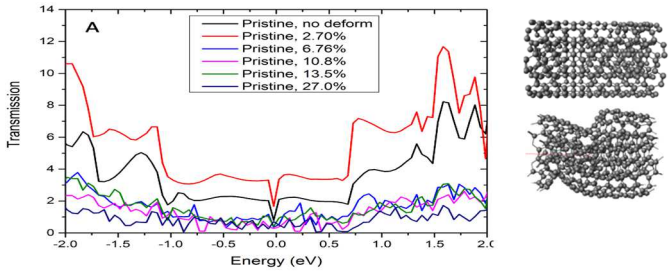

Fig.4. Simulated strain induced change in electronic transmission for pristine DWCNT3 (insert : model of 1 DWCNT before and after 13.5% deformation)

To conclude section III, ballistic electron transport is expected for pristine CNT. However, axially compressed VACNT, which undergoes collapse, as shown in the inset in Figure 4, is shown to have lower transmission and a different mode of transmission. Possibly, at those collapsed and discontinuous regions, non-ballistic electron transfer occurs. The spikes in transmission level suggests that electron hops along a CNT. While it is ideal to obtain MWCNT without defects, defects formation is inevitable under non-ideal condition. The study of this effect is currently under progress.

IV. Design and Characterization of CNTs-based AFWG

This section is dedicated to the design, fabrication and test of a E-band CNTs-based WG. The test structure is described in figure 5. To define the CNTs-based WG, the VACNTs act as metallic walls to connect the gold layers of the top (silicon) and bottom (alumina) substrates (see Step7 in Fig.1). A Grounded Coplanar Waveguide (GCPW) to AFWG transition is designed to generate the WG TE_{10} mode by shorting the I/O GCPW line to the top metallic layer of the WG through two I/O VACNT pillars (see Fig.5). Thus, the induced rotating magnetic field around the pillar is compatible with the magnetic field of the TE_{10} mode and allows the I/O coupling of this mode. Moreover, metallic vias of 150 mm of diameter are introduced according to design rules around the I/O CPW accesses and pillars to avoid parasitic substrate modes.

The AFWG is designed from the bulk equivalent model developed in [18] and implemented in the Finite Element Method software Ansys HFSS. The equivalent bulk material has anisotropic conductivity to account for the fact that charges only move in the direction of the CNTs axis. The conductivity of the CNTs bundle depends on the CNTs' density (D_{CNT}) and is defined by:

$$\sigma_{axial} = \frac{8e^2 v_F}{h(v+j\omega)} D_{CNT} \quad (1)$$

where: ω the angular frequency, $e \approx 1.602 \times 10^{-19}$ C the elementary charge, $t = \tau^{-1}$ the relaxation frequency, v_F the Fermi velocity in CNT, $h \approx 6.626 \times 10^{-34}$ J.s the Plank constant.

According to the equivalent bulk material, we estimate by 3D EM simulations, that the D_{CNT} must be above 10^{13} CNTs/m^2 for obtaining (1) the cutoff frequency of the TE_{10} propagative mode close to the theoretical one defined by the dimensions of the WG and (2) minimal losses in the bandwidth.

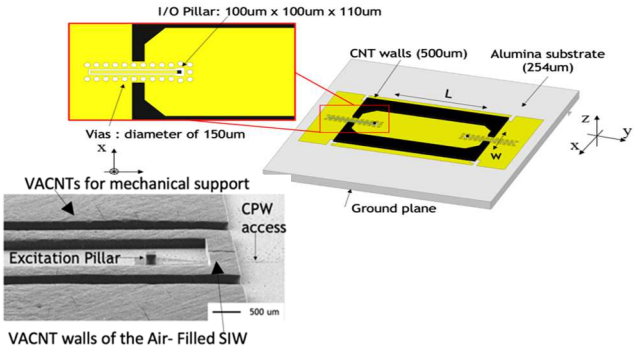

Fig. 5. AFWG without top substrate and I/O accesses – Picture and fabricated test structure

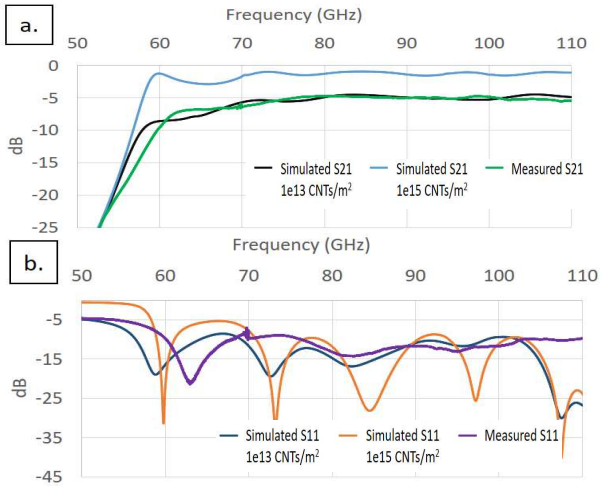

Fig. 6. Measured and Simulated S-parameters

Following this preliminary study, we design the test structure described in figure 5, in the 81-86 GHz operating frequency band. The test WG has a width of 2.7 mm for obtaining a cutoff frequency around 55 GHz, a height of the VACNTs of 110 □m. The width of the CNTs walls is 500□m. The conductivity of the top and bottom gold layers is $4.5*10^7$ S/m and a CNTs density of 10^{15} CNTs/m^2 (equivalent conductivity equal to $2.3*10^5$ S/m according to Eq.1). The fabricated WG (without cover) is shown in Figure 5. The figure

6 shows the measured and simulated S-parameters for a AFWG with a length of 6mm.The measurements are made from 10 MHz to 110 GHz. A Through-Reflect-Line (TRL) calibration is made, the calibration plane is at the probe tips.

For the first time in our knowledge, experimental S-parameters validates the concept of VACNTs-based air-filled WG. The experimental cut-off frequency is close to the theoretical one. The S_{11} is below -10dB in the 81-86 GHz objective-bandwidth, and the S_{21} is about -5dB (including the losses due to the input-output CPW lines and transition). To understand the difference between the experimental insertion losses and the theoretical ones, we run back-EM simulations considering D_{CNT} of 10^{13} CNTs/m^2 instead of 10^{15} CNTs/m^2 initially. As shown in figure 6, the back-simulated S-parameters fit well the measured ones. Moreover, input/output transitions, poor contact resistance, non-controlled compressive strain, air gaps between the VACNTs walls and the top and bottom gold layers can generate insertion losses, as well. We are currently improving such fabrication aspects. At last, the experimental attenuation constant is extracted from two fabricated WG with length of 6 mm and 6.9 mm, thanks to through-line calibration. A value of 0.5 and 0.6 dB/mm is obtained that is comparable to the state-of-the-art described in papers on Silicon Interposer [1], on MnM [4], on Partially Air-Filled MnM [5], on Micro-Machined Coaxial Line [19] that have an attenuation constant of 0.3 to 0.8 dB/mm respectively in the band 110-170 GHz, 50-110 GHz, 80-150 GHz, 110-170 GHz.

V. Conclusion

A dedicated 2.5D technology based on a VACNTs transfer process is developed and applied to fabricate an Air-Filled WG in the E-Band. A first study applying Raman spectroscopy and molecular dynamics is applied to understand the effects of the CNTs compression during the fabrication process. While it is ideal to obtain MWCNT without defects, defects formation is inevitable under actual fabrication conditions. Yet, from the experimental results obtained from measurements on the VACNT based AFWG, it appears that these defects do not notably affect the performances on the RF losses and the overall conductivity of the VACNTs walls. The effect of these compressions on the overall conductivity of the CNTs bundles must be further study. Then, for the first time, an experimental air-filled waveguide based on VACNTs is fabricated and tested with success in the 81-86 GHz band. Measured experimental S-parameters are encouraging and several fabrication aspects (such as higher CNTs density, better I/O transitions and the use of quasi-industrial integration process) can be applied to obtain better performances.

Acknowledgment

This research/project is supported by the National Research Foundation, Singapore and Infocomm Media Development Authority under its Future Communications Research & Development Programme FCP-CNRS-RG-2022-022 and by Ministry of Education, Singapore, under its MOE Tier 2 funding (MOE2018-T2-2-105) and partially funded by MOE grant AcRF TIER 1- 2021-T1-001-064 (RG 55/21).

References

[1] M. Bertrand *et al.*, “Substrate Integrated Waveguides for mm-wave Functionalized Silicon Interposer,” in *2018 IEEE/MTT-S International Microwave Symposium - IMS*, Jun. 2018, pp. 875–878. doi: 10.1109/MWSYM.2018.8439287.

[2] H. J. Tang, W. Hong, G. Q. Yang, and J. X. Chen, “Silicon based THz antenna and filter with MEMS process,” in *2011 International Workshop on Antenna Technology (iWAT)*, Mar. 2011, pp. 148–151. doi: 10.1109/IWAT.2011.5752383.

[3] G. Prigent, A.-L. Franc, M. Wietstruck, and M. Keynak, “Substrate Integrated Waveguide Bandpass Filters implemented on Silicon Interposer for Terahertz Applications,” in *2020 IEEE/MTT-S International Microwave Symposium (IMS)*, Aug. 2020, pp. 595–598. doi: 10.1109/IMS30576.2020.9223781.

[4] M. Bertrand *et al.*, “Integrated Waveguides in Nanoporous Alumina Membrane for Millimeter-Wave Interposer,” *IEEE Microw. Wirel. Compon. Lett.*, vol. 29, no. 2, pp. 83–85, Feb. 2019, doi: 10.1109/LMWC.2018.2887193.

[5] J. Corsi *et al.*, “Partially-Air-Filled Slow-Wave Substrate Integrated Waveguide in Metallic Nanowire Membrane Technology,” in *2020 IEEE/MTT-S International Microwave Symposium (IMS)*, Aug. 2020, pp. 9–12. doi: 10.1109/IMS30576.2020.9223955.

[6] P. Coquet, BK Tay, M. Cometto, D. Baillargeat, S. Bila, K. Frigui, P. Ferrari, E. Pistono, F. Podevin “Interposer and substrate incorporating same”, US Patent granted 11264688, 1st March 2022

[7] H. J. Li, W. G. Lu, J. J. Li, X. D. Bai, and C. Z. Gu, “Multichannel Ballistic Transport in Multiwall Carbon Nanotubes,” *Phys. Rev. Lett.*, vol. 95, no. 8, p. 086601, Aug. 2005, doi: 10.1103/PhysRevLett.95.086601.

[8] CF Siah, LYX Lum, J Wang, SCK Goh, CW Tan, L Hu, P Coquet, H Li, CS Tan, BK Tay, “Development of a CMOS-compatible carbon nanotube array transfer method”, Micromachines 12 (1), 95, 2021

[9] S. Akita, M. Nishio, and Y. Nakayama, "Buckling of carbon nanotubes under axial compression," in *Digest of Papers Microprocesses and Nanotechnology 2005*, 2005, pp. 74-75.

[10] Y. Li, B. Sun, S. Sockalingam, Z. Pan, W. Lu, and T.-W. Chou, "Influence of transverse compression on axial electromechanical properties of carbon nanotube fibers," *Materials & Design,* vol. 188, p. 108463, 2020/03/01/ 2020.

[11] M. S. Dresselhaus, G. Dresselhaus, R. Saito, and A. Jorio, "Raman spectroscopy of carbon nanotubes," *Physics Reports,* vol. 409, no. 2, pp. 47-99, 2005/03/01/ 2005.

[12] A. Jorio and R. Saito, "Raman spectroscopy for carbon nanotube applications," *Journal of Applied Physics,* vol. 129, no. 2, p. 021102, 2021.

[13] M. Dresselhaus, A. Jorio, A. Souza Filho, and R. Saito, "Defect characterization in graphene and carbon nanotubes using Raman spectroscopy," *Philosophical transactions. Series A, Mathematical, physical, and engineering sciences,* vol. 368, pp. 5355-77, 12/01 2010.

[14] A. Sears and R. C. Batra, "Buckling of multiwalled carbon nanotubes under axial compression," *Physical Review B,* vol. 73, no. 8, p. 085410, 02/16/ 2006.

[15] U. A. Joshi, S. C. Sharma, and S. P. Harsha, "Effect of carbon nanotube orientation on the mechanical properties of nanocomposites," *Composites Part B: Engineering,* vol. 43, no. 4, pp. 2063-2071, 2012/06/01/ 2012.

[16] Available: www.scm.com

[17] K. Chenoweth, A. C. T. van Duin, and W. A. Goddard, "ReaxFF Reactive Force Field for Molecular Dynamics Simulations of Hydrocarbon Oxidation," *The Journal of Physical Chemistry A,* vol. 112, no. 5, pp. 1040-1053, 2008/02/01 2008.

[18] P. Franck, D. Baillargeat, and B. K. Tay, “Mesoscopic Model for the Electromagnetic Properties of Arrays of Nanotubes and Nanowires: A Bulk Equivalent Approach,” *IEEE Trans. Nanotechnol.*, vol. 11, no. 5, pp. 964–974, Sep. 2012, doi: 10.1109/TNANO.2012.2209457.

[19] F. David, M. Chatras, C. Dalmay, L. Lapierre, L. Carpentier, and P. Blondy, “Surface-Micromachined Rectangular Micro-Coaxial Lines for Sub-Millimeter-Wave Applications,” *IEEE Microw. Wirel. Compon. Lett.*, vol. 26, no. 10, pp. 756–758, Oct. 2016, doi: 10.1109/LMWC.2016.2604867.